

# Design of Dual-Band and Dual-Polarized Microstrip Antenna for Applications on HAPs

Lucas S. Pereira, Marcos V. T. Heckler and Cleiton Lucatel

**Abstract**—This paper presents the design of a dual-band microstrip antenna with dual polarization characteristic for high altitude platforms (HAPs). The antenna has two isolated ports and is suitable for terminals with receiving and transmitting functions operating simultaneously. The element is designed for operation at 5.8 and 7 GHz with 100 MHz bandwidth in each band. The antenna geometry and its main design parameters are presented and discussed in the paper. Numerical and experimental results show that this radiator exhibits good performance in terms of impedance matching and circular polarization purity.

**Keywords**—Dual-Band; Dual-Polarized; Microstrip Antenna.

## I. INTRODUCTION

Microstrip and printed antennas have been used widely in wireless systems such as wireless local access network (WLAN), mobile communications and global positioning satellite systems (GNSS).

Among other advantages, microstrip antennas are very suitable for integration into arrays and can be easily integrated with discrete components, such as low-noise amplifiers, mixers and filters, which are interesting traits for the development of all variations of adaptive antennas [1]. As a special case, retro-directive antenna arrays exhibit the ability to resend signals to the same direction where they have been received from [2]. Traffic control and collision avoidance systems are examples in which retro-directive antenna arrays find future application [3], [4].

Dual-band antennas have been studied widely. The most used techniques are stacking of patches [5]-[7] and coplanar configurations [8]-[9]. However, none of these contributions analyze antennas with two isolated ports, which is the main contribution reported in this paper. The antenna should be suitable for integration into a retro-directive array to be installed on a high-altitude platform (HAP). For this purpose, it should exhibit dual-band and dual-polarized behavior. Additionally, it should work as a receiving (Rx) and transmitting (Tx) antenna simultaneously. For this reason, the proposed geometry presents two ports with large isolation between them. According to the European regulations for fixed satellite systems (ECA Table) [8], the HAP should be designed to work as Rx at 5.8 GHz and as Tx at 7.0 GHz. At both frequencies, the signal to be retransmitted has maximum bandwidth of 100 MHz, which means 1.72% bandwidth at 5.8 GHz and 1.43% at 7.0 GHz. Dual polarization is used to improve isolation between the uplink and the downlink channels, whereby the antenna should be right-handed

circularly polarized (RHCP) at 5.8 GHz and left-handed circularly polarized (LHCP) at 7.0 GHz.

In the next section, the geometry of the proposed antenna is depicted. Section III presents the experimental validation of the built prototype.

## II. DUAL-BAND AND DUAL-POLARIZED MICROSTRIP ANTENNA

The stack-up considered for the construction of the designed antenna is shown in Figure 1. The multilayer structure is composed of three low-loss microwave laminates TACONIC TLA-6 with dielectric constant of 2.62 and loss tangent of 0.0012. The top laminate supports the patch that is tuned to operate in the higher band, whereas the radiator that resonates at 5.8 GHz is printed on the middle laminate. An air layer has been added between the patches in order to increase the bandwidth in the top band and to allow soldering the via to the bottom patch prior to the final assembly. The two lower laminates are glued with TACONIC FastRise prepreg with thickness  $h_{glue} = 0.21$  mm, dielectric constant of 2.75 and loss tangent of 0.0014. Both patches have the shape of a square with truncated corners and are fed by two independent microstrip lines. The connection between the patches and the lines is done by means of metallic vias.

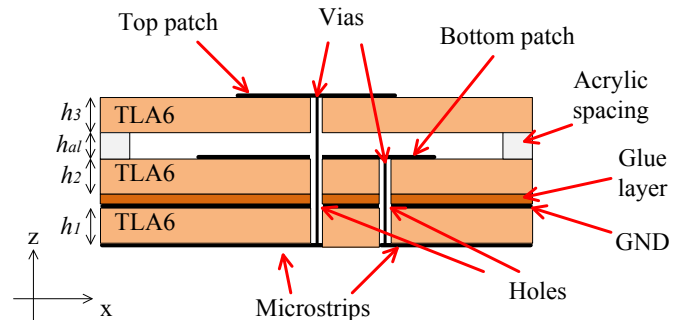


Fig. 1 - Cross sectional view of the dual-band antenna.

The schematic top view of the antenna is shown in Figure 2. In order to avoid electrical connection between both patches, a hole was drilled in the bottom patch to isolate it from the via that feeds the top patch. The axial ratio for both radiators can be optimized for the desired frequencies by adjusting the side lengths  $L_{sup}$  and  $L_{inf}$  and the truncation dimensions  $x_{sup}$  and  $x_{inf}$  for the top and bottom patches, respectively.

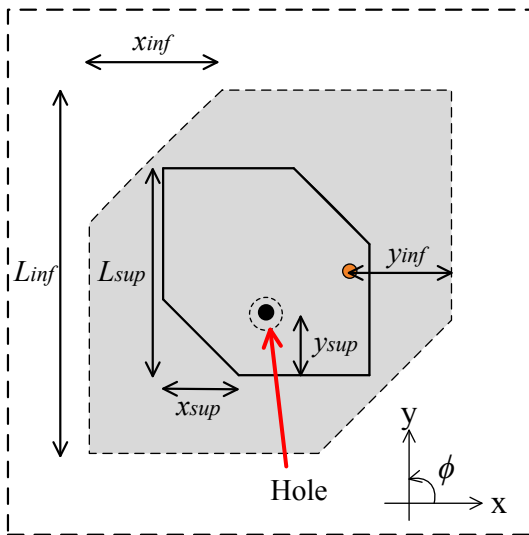


Fig. 2 - Schematic top view of the two square patches.

Due the interaction between the both patches, which disturbs the input impedance in comparison to single patches, and the fact that the via that connect the top patch to the respective feed line is long and introduces a strong inductive component to the input impedance, the impedance matching for this structure cannot be realized by adjusting the  $y_{sup}$  and  $y_{inf}$  parameters only as in ordinary square patches with truncated corners. In the present case, this is done by the open-ended single stub technique. The schematic view of the antenna feeding system is shown in Figure 3. The parameters  $d_{inf}$  and  $l_{inf}$  can be optimized to perform impedance matching at the lower band of operation. Similarly,  $d_{sup}$  and  $l_{sup}$  can be used for impedance matching at the upper band.

The optimization of the antenna parameters has been conducted in the electromagnetic simulator Ansys HFSS [11].

In order to improve isolation, a quarter-wave open-ended stub tuned at 5.8 GHz has been connected to the line that feeds the top patch. By transmission line theory, one can derive that this stub acts as a short circuit at 5.8 GHz in the location of its connection to the feed line. As a result, the magnitude of the reflection coefficient is nearly 0 dB at this frequency, hence producing large isolation between the ports. In the top band, this quarter-wave long stub introduces an additional inductive reactance in the antenna input impedance, which needs to be taken into account during the impedance matching procedure. In the same way, a quarter-wave long stub tuned at 7.0 GHz was connected to the feed line that feeds the bottom patch. Short circuit is produced at 7.0 GHz and an additional capacitive reactance is introduced in the input impedance at 5.8 GHz. The optimized dimensions  $d_{bot}$ ,  $l_{bot}$ ,  $d_{top}$  and  $l_{top}$  for the two decoupling stubs as well as for the other project variables are given in Table I.

### III. EXPERIMENTAL CHARACTERIZATION

A prototype was built and is shown in Figure 4. The comparison between simulated and measured S-parameters is shown in Figures 5 and 6 for the lower and higher bands, respectively. One can see that large isolation between the Rx and Tx ports is obtained, as well the good impedance matching.

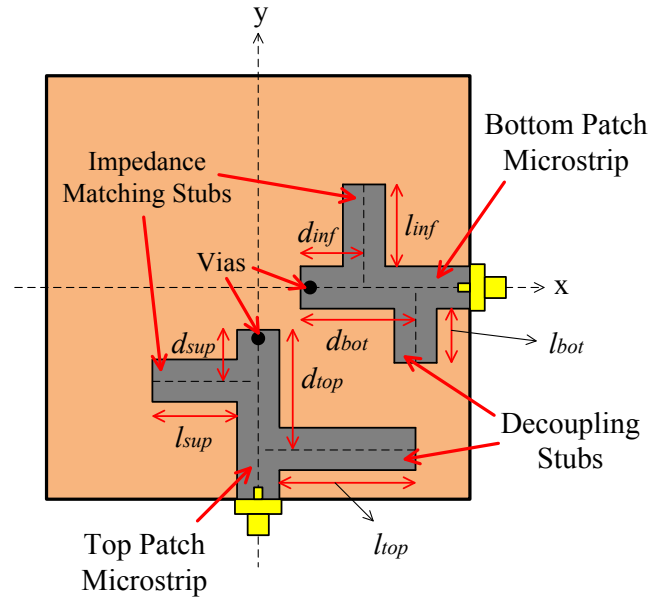
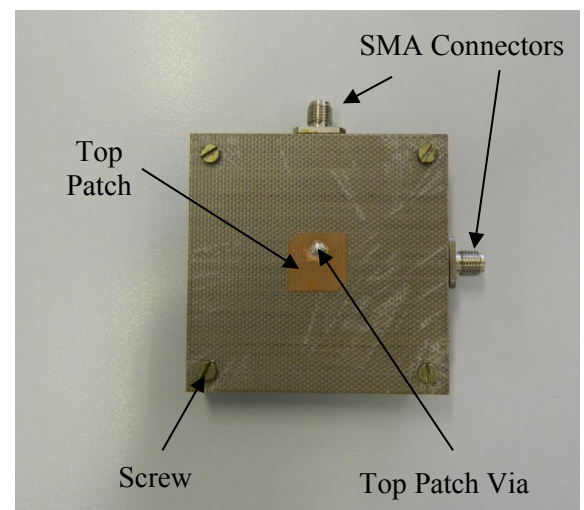


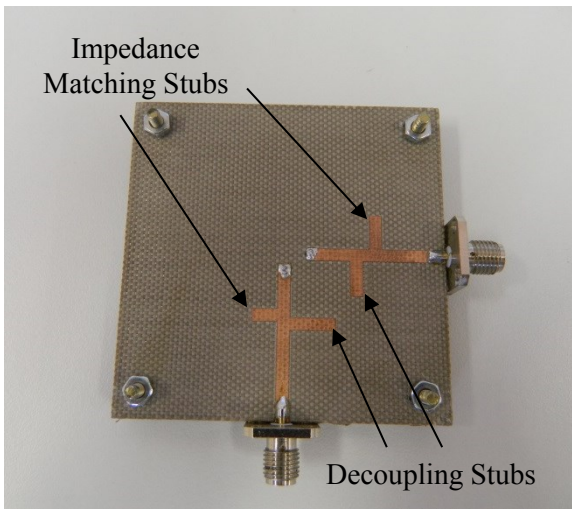
Fig. 3 - Schematic view of the antenna feeding system.

TABLE I. OPTIMIZED ANTENNA DIMENSIONS.

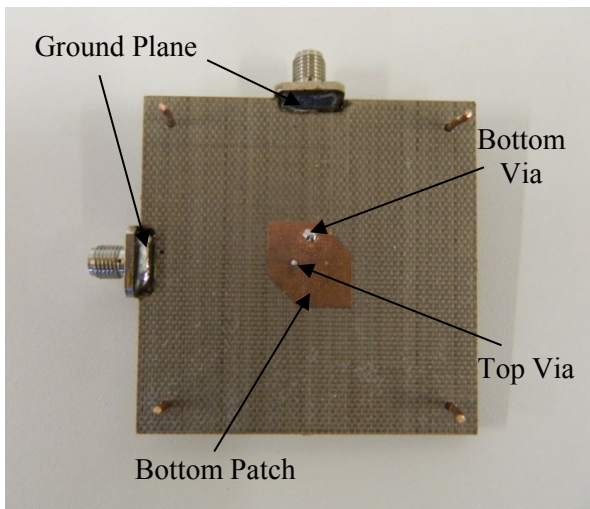
Parameter	Value (mm)	Parameter	Value (mm)
$L_{sup}$	13.63	$h_3$	1.96
$y_{sup}$	2.90	$d_{inf}$	8.50
$x_{sup}$	2.49	$l_{inf}$	4.50
$L_{inf}$	15.11	$W_s$	2.82
$y_{inf}$	5.00	$d_{sup}$	8.40
$x_{inf}$	5.63	$l_{sup}$	6.50
$d_{hole}$	2.00	$d_{bot}$	12.00
$h_1$	1.02	$l_{bot}$	6.50
$h_2$	1.96	$d_{top}$	10.00
$W_i$	2.82	$l_{top}$	8.40
$h_{al}$	1.40	$h_{glue}$	0.21



(a)



(b)



(c)

Fig. 4 - Dual-band and dual-polarized microstrip antenna: (a) Top view of the top patch; (b) Bottom view with the feed system of the built antenna; (c) Top view of the bottom patch.

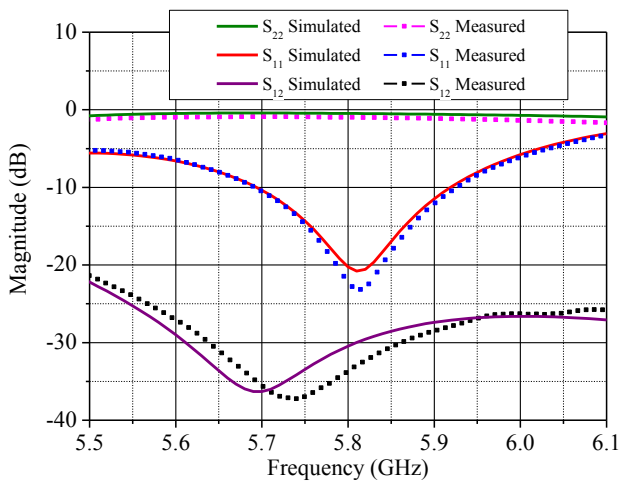


Fig. 5 - Simulated and measured S-parameters in the lower band (the curves for  $S_{12}$  and  $S_{21}$  are coincident due to reciprocity).

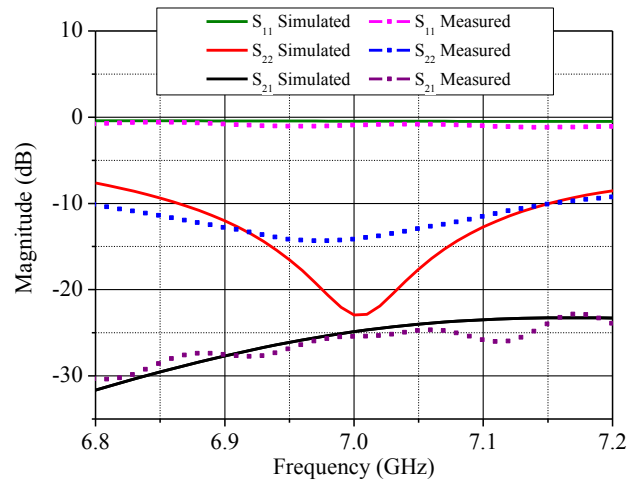


Fig. 6 - Simulated and measured S-parameters in the upper band (the curves for  $S_{12}$  and  $S_{21}$  are coincident due to reciprocity).

The predicted radiation properties in the software HFSS at the lower and the higher band for this antenna are shown in Figures 7, 8, 9 and 10, respectively. The axial ratio (AR) behavior for the antenna in the boresight is optimum at the desired center frequency and satisfies the bandwidth specification, if the criterion  $AR < 3$  dB is considered. The antenna exhibits a gain in the boresight of 5.67 dBi for the lower band and 3.94 dBi for the higher band.

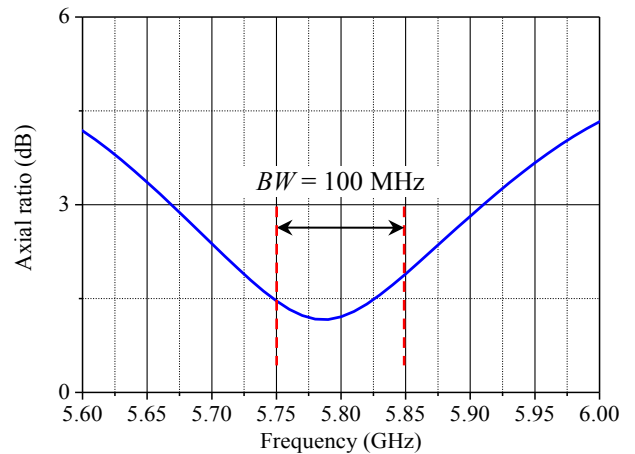


Fig. 7 - Axial ratio in the boresight versus frequency for the lower band.

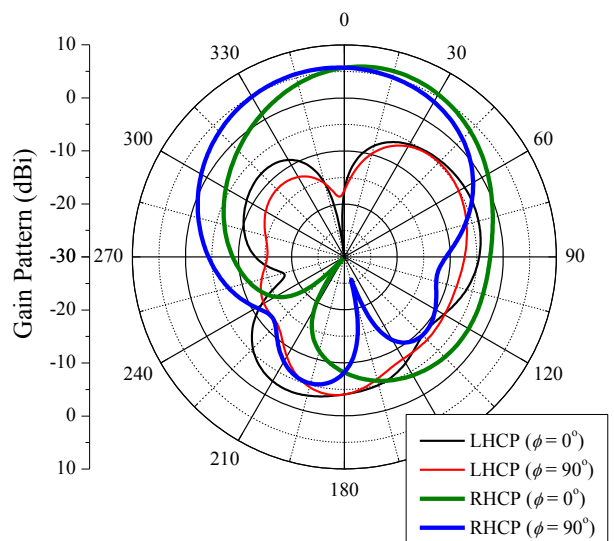


Fig. 8 - Gain pattern at 5.8 GHz.

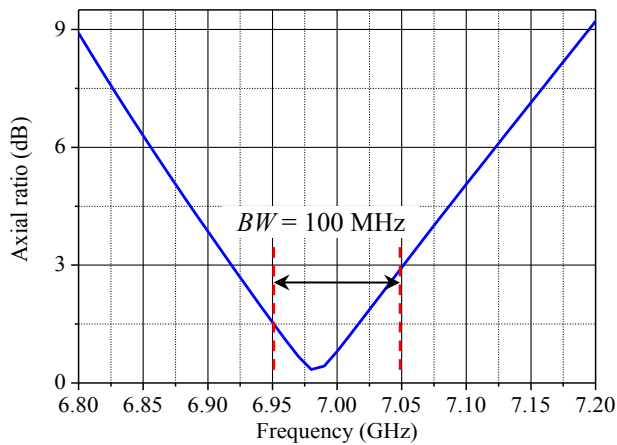


Fig. 9 - Axial ratio in the boresight versus frequency for the upper band.

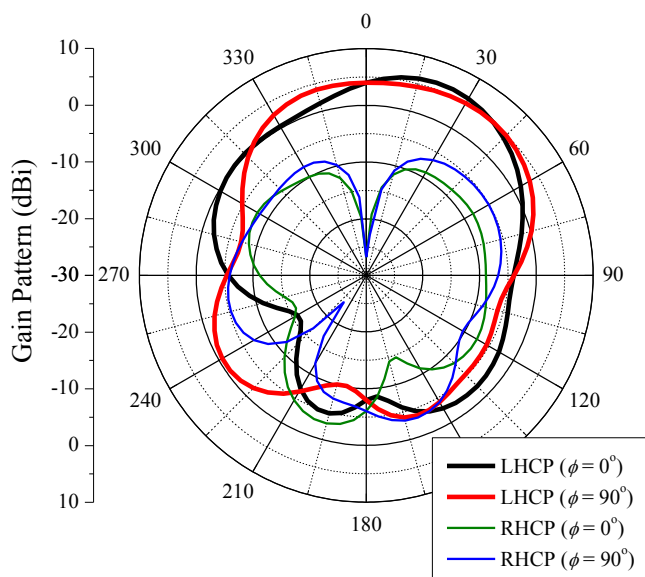


Fig. 10 - Gain pattern at 7 GHz.

IV. CONCLUSIONS

This paper presented the design procedure and experimental validation of a geometry of a microstrip antenna that can be operated in two bands with circular polarization in both bands. It has been verified that good agreement between measured and simulated S-parameters has been obtained. The desired radiation characteristics were achieved.

The antenna feed system is composed of two decoupling stubs to provide the high isolation between the bands of operation and two single stubs open-ended to realize the impedance matching of the radiator. Two vias were employed to connect the two patches to the microstrips.

Large isolation between the Rx and Tx ports has been obtained experimentally. Considering the center frequencies only, the isolation is -30.5 dB at 5.8 GHz and -25 dB at 7.0 GHz. This proves that the proposed antenna concept serves as a diplexer and a first filtering device between the Tx and Rx channels. This feature reduces strongly the requirements of

filtering out the Tx band by the front-end circuitry of the receiver. Therefore, the proposed antenna is a strong candidate to compose an antenna array for high altitude platforms, since the good radiation characteristics have been obtained, as well as good isolation between the two bands of operation.

ACKNOWLEDGEMENTS

The authors would like to thank to the Brazilian National Research and Development Council (CNPq) for the partial support under grant 484406/2012-4.

REFERENCES

- [1] R. Garg, P. Bhartia, I. Bahl, A. Ittipiboon, *Microstrip Antenna Design Handbook*, Artech House, 2001.
- [2] R. Y. Miyamoto and T. Itoh, "Retrodirective arrays for wireless communications," *IEEE Microwave Magazine*, vol. 3, no. 1, pp. 71-79, Mar. 2002.
- [3] C. Shyh-Jong and K. Chang. "A Retrodirective Microstrip Antenna Array". *IEEE Transactions on Antennas and Propagation*, Vol. 46, No. 12, December 1998, pp. 1802-1809.
- [4] L. Kevin M. K. H., M. Ryan Y. and I. Tatsuo. "Moving Forward in Retrodirective Antenna Arrays". *IEEE Potentials*. August/September 2003.
- [5] B. Huang, Y. Yao and Z. Feng. "A Novel Wide Beam Dual-Band Dual-Polarization Stacked Microstrip Dielectric Antenna". *Microwave and Millimeter Wave Technology*, 2007, pp. 1-4, April 2007.
- [6] X. Sun, Z. Zhang and Z. Feng. "Dual-Band Circularly Polarized Stacked Annular-Ring Patch Antenna for GPS Application". *IEEE Antennas and Wireless Propagation Letters*, Vol. 10, pp. 49-52, January 2011.
- [7] R. K. Vishwakarma. "Design of rectangular stacked microstrip antenna for Dual-band". *International Conference on Emerging Trends and Photonic Devices & Systems*, pp. 22-24, Dec. 2009.
- [8] M. Noghabaei, S. K. A. Rahim and M. I. Sabran. "Dual Band Single Layer Microstrip Antenna with Circular Polarization for WiMAX Application". *6th European Conference on Antennas and Propagation (EuCAP)*, pp. 1996-1999, March 2012.
- [9] F. Yang and Y. R. Samii. "A Single Layer Dual Band Circularly Polarized Microstrip Antenna for GPS Application". *IEEE Antennas and Propagation Society International Symposium*, Vol. 4, pp. 720-723, 2002.
- [10] Electronic Communication Committee, *The European table of frequency allocations and applications in the frequency range 8.3 kHz to 3000 GHz (ECA TABLE)*, available at <http://www.erodocdb.dk/docs/doc98/official/pdf/ERCRep025.pdf>.
- [11] Ansys Corporation, *Ansys HFSS user's guide*, version 15.0.

Lucas Santos Pereira, Marcos Vinicio Thomas Heckler and Cleiton Lucatel, Telecommunications Engineering, Federal University of Unipampa, Alegrete-RS, Brazil, E-mails: lucaspereira, marcos.heckler, cleiton.lucatel@unipampa.edu.br. This work was partially supported by CNPq (484406/2012-4).